Generalized Huang-Rhys factors for molecular aggregates

Generalized Huang-Rhys factors for molecular aggregates

Maxim F. Gelin[1], Erling Thyrhaug[1], Lipeng Chen[1],
Raffaele Borrelli[2], and Wolfgang Domcke[1]
[1]*Department of Chemistry, Technische Universität München, D-85747 Garching, Germany*
[2]*DISAFA, Università di Torino, I-10095 Grugliasco, Italy*

Abstract

Stimulated Raman experiments of molecular aggregates often reveal remarkably different spectral structure than other vibrational spectroscopies. Clear examples of such discrepancies can be found in photosynthetic pigment-protein complexes, but also *e.g.* in a wide range of artificial J-aggregates. Using time-domain techiques in these settings, one often observe extremely sparse vibrational spectra containing predominantly low-frequency modes of surprisingly large intensity, rather than the rich spectrum of modes found using frequency-domain techniques such as hole burning and Raman spectroscopy. Thus, it appears that a mechanism is required which selectively enhances the oscillator strength of a small sub-set of vibronic transitions under typical stimulated Raman conditions in coupled molecular complexes .

In this work, we address this issue by exploring how pigment-localized vibrations couple to the excitonic states of molecular aggregate systems. In particular, we analyze how this vibronic coupling changes as a function of excitonic delocalization, and what the consequences are for spectral observables.

To comprehend this phenomenon, we introduce the concept of a generalized Huang-Rhys factor for molecular aggregates consisting of any number of monomers with arbitrary number of vibrational modes. We derive compact analytical expression for this quantity, and established two conditions – #1 and #2 – which must be simultaneously fulfilled in order to observe strong coupling of the excitonic and vibrational degrees of freedom. We illustrate the remarkably strong effect of such vibronic coupling by numerical simulations of absorption and resonance Raman spectra of a two-mode model dimer.

I. INTRODUCTION

In the simplest quantum mechanical treatments of light-matter interactions, photons are absorbed and emitted as prescribed by vertical transitions between system eigenstates – resulting in spectra composed of sharp spectral lines at frequencies directly corresponding to the energy-differences between these eigenstates. While this picture is approximately valid for *e.g.* many cold atomic gases, the situation for molecular aggregates embedded in dissipative condensed-phase environments is far more complicated. The hundreds of vibrational modes present in these systems – intramolecular and in the surrounding bath – result in a high density of states, and nonadiabatic effects, vibrational relaxation, electronic dephasing and static disorder all contribute to the optical response of the aggregate. As a result, transitions are manifested as broad and asymmetric vibronic bands (in the frequency domain) or complicated, often oscillatory signals (in the time domain) [1–3].

In many important systems one might suspect that some significant simplifications could nevertheless be made to this complicated picture, as electron-vibrational coupling is often weak. In particular, one could naively assume that vibrational modes are, to good approximation, decoupled from the electronic degrees of freedom, and that the spectroscopic signals can be grasped in terms of a pure excitonic picture. The pigment-protein-complexes (PPCs) found in natural photosynthesis, largely based on assemblies of small-Huang-Rhys factor chlorophylls [4–6], are an important class of systems where one might be tempted to apply such an approximation.

It is well known, however, that this simple picture does not hold in general: The electrostatic interaction between chromophores in such aggregates results in the formation of delocalized excitonic eigenstates, and vibrational modes that couple only weakly to the electronic states in isolated pigment may experience substantially different coupling to the states in the coupled multi-pigment system. It has been pointed out that such vibronic mixing effects, appearing under suitable conditions in electronically coupled systems, could be responsible for the relatively strong oscillatory signals observed in the ultrafast kinetics of a wide range of biological and artificial molecular aggregates [7–16] (see also more recent papers [17–22] and references therein).

Beyond spectroscopy, in the context of electronic energy and charge transfer processes, the significance of resonant vibrations has been widely appreciated, and a reasonable qualitative

understanding has been achieved [23–32]. Due to the complexity of the problem, however, the influence of exciton-vibrational coupling on the photophysics of molecular aggregates has been largely studied by numerical simulations of specific, usually relatively simple, models (see papers [7–32] and reviews [33–35]).

Here we extend this work on aggregates of molecular chromophores – presenting a general analytical analysis of weakly coupled pigment-localized vibrations in excitonically coupled molecular aggregates of arbitrary size and number of vibrational modes. We introduce a generalized Huang-Rhys factor for multi-pigment aggregates, and establish the specific conditions under which excitonic and vibrational degrees of freedom become strongly mixed and vibronic transitions gain intensity by redistribution of the total oscillator strength. We substantiate the analytical results by numerical simulations of linear absorption and resonance Raman spectra of a model dimer, using typical parameters found in pigment-protein complexes.

Note that $\hbar = 1$ throughout the paper.

II. STARTING EQUATIONS

We consider a generic molecular aggregate consisting of N_e chromophores placed in a dissipative environment (solvent). Each chromophore is modeled as an electronic two-level system possessing N_v vibrational modes. The Hamiltonian of this aggregate in site representation can be represented as a sum of the excitonic Hamiltonian, vibrational Hamiltonian, and their coupling [36, 37]:

$$H = H_e + H_v + H_{ev}, \tag{1}$$

$$H_e = \sum_{k,k'}^{N_e} E_{kk'} B_k^\dagger B_{k'}, \tag{2}$$

$$H_v = \sum_{k=1}^{N_e} \sum_{\alpha=1}^{N_v} \frac{\Omega_{k\alpha}}{2} \left(P_{k\alpha}^2 + X_{k\alpha}^2 \right), \tag{3}$$

$$H_{ev} = \sum_{k=1}^{N_e} \sum_{\alpha=1}^{N_v} \Omega_{k\alpha} \kappa_{k\alpha} B_k^\dagger B_k X_{k\alpha}. \tag{4}$$

Here, the operators $B_k^\dagger$ and B_k create excitation on site k and obey the Pauli commutation rules $[B_k, B_{k'}^\dagger] = \delta_{kk'}(1 - 2B_k^\dagger B_{k'})$. $E_{kk'}$ are the site energies ($k = k'$) and couplings ($k \neq k'$), and $X_{k\alpha}$, $P_{k\alpha}$ and $\Omega_{k\alpha}$ are the dimensionless positions, dimensionless momenta, and

frequencies of the harmonic mode α of the chromophore k. The small parameters $\kappa_{k\alpha}$ control the strength of the intra-chromophore electron-vibrational coupling in individual chromophores.

The Hamiltonian H_e can be diagonalized by the orthogonal transformation $\mathcal{O}$

$$E_{kk'} = \sum_{n=1}^{N_e} \mathcal{O}_{kn} \varepsilon_n \mathcal{O}_{nk'}$$

Introducing the new excitonic operators

$$C_n = \sum_{k=1}^{N_e} \mathcal{O}_{nk} B_k.$$

and applying the transformation $\mathcal{O}$ to the Hamiltonian (1), we obtain the equivalent Hamiltonian $\mathcal{H}$ in the excitonic representation [38]:

$$\mathcal{H} = \mathcal{O} H \mathcal{O}^\dagger = \mathcal{H}_e + \mathcal{H}_v + \mathcal{H}_{ev} \tag{5}$$

where

$$\mathcal{H}_e = \sum_{n=1}^{N_e} \varepsilon_n C_n^\dagger C_n, \tag{6}$$

$$\mathcal{H}_{ev} = \sum_{k,n,n'=1}^{N_e} \sum_{\alpha=1}^{N_v} A_{k\alpha}^{nn'} C_n^\dagger C_{n'} X_{k\alpha}, \tag{7}$$

$$\mathcal{H}_v = H_v \tag{8}$$

and

$$A_{k\alpha}^{nn'} = \Omega_{k\alpha} \kappa_{k\alpha} \mathcal{O}_{nk} \mathcal{O}_{n'k}.$$

Note that in the excitonic representation the system now possesses both diagonal $A_{k\alpha}^{nn}$ and off-diagonal ($A_{k\alpha}^{nn'}$, $n \neq n'$) exciton-vibrational couplings.

III. EIGENVALUES OF THE EXCITONIC HAMILTONIAN

In order to clarify how the exciton-vibrational coupling in molecular aggregates depends on the parameters of Hamiltonians (1) and (5), we analytically evaluate the eigenvalues of the Hamiltonian $\mathcal{H}$ in the limit of weak pigment-localized vibrational coupling. This limit is relevant for biological PPCs where, for instance, the total vibrational Huang-Rhys factor $S =$

$\sum_{k\alpha} \kappa_{k\alpha}^2$ for the bacterial photosynthetic reaction center [4] and the Fenna–Matthews–Olson complex [5, 6] is ≈ 0.3.

We introduce the eigenfunctions and eigenvalues of the purely excitonic and vibrational Hamiltonians:

$$\mathcal{H}_e \left|r\right\rangle = \varepsilon_r \left|r\right\rangle , \;\; \mathcal{H}_v \left|\lambda\right\rangle = \chi_\lambda \left|\lambda\right\rangle \tag{9}$$

which are readily available analytically. $\mathcal{H}_e$ and $\mathcal{H}_v$ commute, and we can write:

$$(\mathcal{H}_e + \mathcal{H}_v) \left|r\right\rangle \left|\lambda\right\rangle = (\varepsilon_r + \chi_\lambda) \left|r\right\rangle \left|\lambda\right\rangle . \tag{10}$$

We denote the eigenfunctions and eigenvalues of the total Hamiltonian as $|r\lambda\rangle$ and $\mathcal{E}_{r\lambda}$,

$$\mathcal{H} \left|r\lambda\right\rangle = \mathcal{E}_{r\lambda} \left|r\lambda\right\rangle . \tag{11}$$

Then $\mathcal{E}_{r\lambda}$ can be found analytically in the leading, quadratic in $\kappa_{k\alpha}$ order. The detailed derivation is given in Appendix A. Here we cite the final result:

$$\mathcal{E}_{r\lambda} = \varepsilon_r + \chi_\lambda - \sum_{k,m=1}^{N_e} \sum_{\alpha=1}^{N_v} S_{k\alpha}^{rm} \left[(1 + 2n_{k\alpha}^{\lambda})\omega_{rm} + \Omega_{k\alpha}\right] + O(\kappa_{k\alpha}^4) \tag{12}$$

where

$$\omega_{rm} = \varepsilon_r - \varepsilon_m \tag{13}$$

are the excitonic transition frequencies and

$$n_{k\alpha}^{\lambda} = \langle\lambda| a_{k\alpha}^{\dagger} a_{k\alpha} \left|\lambda\right\rangle \tag{14}$$

are the vibrational occupation numbers (the creation and annihilation operators, $a_{k\alpha}^{\dagger}$ and $a_{k\alpha}$, are expressed in terms of the dimensionless positions $X_{k\alpha}$ and momenta $P_{k\alpha}$ through Eq. (A6)). As outlined below, the factor

$$S_{k\alpha}^{rm} = \frac{(A_{k\alpha}^{rm})^2}{2(\Omega_{k\alpha}^2 - \omega_{rm}^2)} \tag{15}$$

can be regarded as a Huang-Rhys factor generalized to multi-pigment systems. In the special case of a dimer ($N_e = 2$) with a single vibrational mode per monomer ($N_v = 1$) this reduces to a well known result [39].

IV. GENERALIZED HUANG-RHYS FACTOR

Eqs. (12) and (15) are the main analytical result of the present work. It is clear that the factor $S^{rm}_{k\alpha} \sim \kappa^2_{k\alpha}$ defined in Eq. (15) controls the exciton-vibrational coupling in the molecular aggregate. To elucidate how this coupling constant depends on the parameters specifying the aggregate, it is helpful to consider two cases.

A. Single chromophore

In this case, $N_e = 1$ and the Hamiltonian (5) describes a collection of shifted harmonic oscillators. This system can be treated analytically for any $\kappa_{k\alpha}$, but for consistency we remain with the perturbative treatment. Adopting Eq. (12) for the case of a single chromophore, we set

$$k = m = r = 1,\ \mathcal{O}_{rk} = 1,\ \omega_{rm} = 0,$$

and obtain

$$S^{11}_{1\alpha} = \kappa^2_{k\alpha}/2 \tag{16}$$

This is the standard Huang-Rhys factor of the chromophore [40], substantiating our interpretation of the vibronic coupling constant $S^{rm}_{k\alpha} \sim \kappa^2_{k\alpha}$ as a generalized Huang-Rhys factor.

B. Molecular aggregate

For a molecular aggregate the situation is dramatically different from that of the single chromophore. While $S^{rm}_{k\alpha}$ remains proportional to $\kappa^2_{k\alpha}$, significant dependencies on other parameters appear. Due to these dependencies, the exciton-vibrational coupling in molecular aggregates can become strong even if the coupling in the individual monomers is weak ($\kappa^2_{k\alpha} \ll 1$). Investigating the expression Eq. (15) two conditions appear crucial to achieving strong coupling:

1. Condition #1

For $N_e > 1$, the generalized Huang-Rhys factor of Eq. (15) possesses a resonant denominator. Hence the strongest exciton-vibrational coupling is expected when the excitonic

transition frequency and the vibrational mode frequency are similar,

$$|\omega_{rm}| \approx |\Omega_{k\alpha}|. \tag{17}$$

In this case exciton-vibrational coupling becomes substantial, giving rise to strong mixing of excitonic and vibrational degrees of freedom. If, on the other hand, $|\Omega_{k\alpha}| \gg |\omega_{rm}|$ then $S_{k\alpha}^{rm} = \mathcal{O}_{rk}^2\mathcal{O}_{mk}^2\kappa_{k\alpha}^2/2$. As a result, the strong-coupling regime cannot be reached for vibrational modes with frequencies large relative to the excitonic splitting - although the actual coupling may differ from that of the individual chromophore due to the redistribution of the coupling strength by the $\mathcal{O}_{rk}^2\mathcal{O}_{mk}^2$ factors. Note that higher-order resonances ($|\omega_{rm}| \approx j|\Omega_{k\alpha}|$ for $j > 1$), do not contribute to $\mathcal{E}_{r\lambda}$ in the small $\kappa_{k\alpha}$ regime investigated here. If $|\omega_{rm}| = |\Omega_{k\alpha}|$, the unperturbed excitonic and vibrational energy levels become degenerate and simple perturbation theory breaks down.

2. Condition #2

Condition #1 is necessary, but not sufficient for strong exciton-vibrational coupling. In addition the site energy differences must be of the order of the inter-site couplings,

$$|E_{kk} - E_{k'k'}| \simeq |E_{kk'}|, \;\; k \neq k'. \tag{18}$$

This requirement reflects that, in the opposite limit $|E_{kk} - E_{k'k'}| \gg |E_{kk'}|$, the dynamics becomes almost adiabatic ($\mathcal{O}_{rk} \approx \delta_{rk}$) and the Hamiltonians H and $\mathcal{H}$ virtually coincide. In this case, $A_{k\alpha}^{nn'}$ becomes diagonal,the generalized Huang-Rhys factor reduces to $S_{k\alpha}^{rm} = \delta_{rk}\delta_{mk}\kappa_{k\alpha}^2/2$ – *i.e.* a collection of the Huang-Rhys factors of the isolated pigments, and strong exciton-vibrational coupling cannot be realized.

In summary, in order to reach the strong coupling regime it is strictly necessary to simultaneously fulfill both conditions #1 and #2. If either or both of the conditions are not fulfilled, $S_{k\alpha}^{rm} \simeq \kappa_{k\alpha}^2/2$ – the Huang-Rhys factor of the collection of isolated chromophores.

V. NUMERICAL ILLUSTRATION

To substantiate the above analytical results and principles, we simulate the linear absorption $I(\omega)$ and resonance Raman $R(\omega)$ spectra of a model molecular dimer at room temperature. Our aim is to demonstrate how vibrational-electronic coupling modulates optical

spectra, and how relatively modest changes in model parameters can lead to substantially different results (as implied by the conditions #1 and #2). Rather than accurate modelling of a specific optical response, we are here concerned with general features of the model. In order to most clearly highlight these, we make several simplifications and adopt particular choices of parameters. Most notably, we neglect vibrational relaxation and account for the environment only through optical dephasing. We assume relatively slow dephasing at $\tau = 200$ fs, which allows all transitions in the absorption spectrum $I(\omega)$ to be clearly distinguishable. Similarly, the lineshapes in the resonance Raman spectra $R(\omega)$ are Lorenzian with a width 2000 fs^{-1}.

The resulting purely excitonic dimer system consists of two coupled monomers with site energies ϵ_1 and ϵ_2. We set $\epsilon_1 = 0$, and systematically vary ϵ_2 (and thus the monomer energy splitting) in order to emulate the different site-energies found in molecular aggregates. The dipole-dipole coupling between sites is fixed to $\Delta \equiv E_{12} = 98$ cm^{-1} - a fairly typical magnitude observed in many biological aggregates, *e.g.* between bacteriochlorophyll sites 1 and 2 in the Fenna-Matthews-Olson PPC [42, 43]). The vibrationless dimer thus has two excitonic states,

$$E_1 = \frac{1}{2}\big(\epsilon_2 - \delta_\epsilon\big), \;\; E_2 = \frac{1}{2}\big(\epsilon_2 + \delta_\epsilon\big), \tag{19}$$

split by an energy:

$$\delta_\epsilon = \sqrt{\epsilon_2^2 + 4\Delta^2}.$$

To this excitonic system we introduce a low-frequency and a high-frequency vibrational mode at each monomer site. We choose representative bacteriochlorophyll vibrational frequencies [41] $\Omega_1 = 195$ cm^{-1} and $\Omega_2 = 724$ cm^{-1}. The electron-vibrational couplings are $\kappa_1 = 0.289$ and $\kappa_2 = 0.226$, respectively – again typical of bacteriochlorophylls. The dimer is thus described by the Hamiltonian of Eq. (1), with $N_e = 2$ and $N_v = 2$ and having $N_e \times N_v = 4$ vibrational modes.

While it is clear from Eq. (12) that the system eigenstates depend on the interaction between excitonic and vibrational degrees of freedom, the consequences in terms of observables $I(\omega)$ and $R(\omega)$ are not obvious and their detailed exploration requires numerical simulations. For this dimer system, the transition dipole moment operators are defined as [36, 37]

$$Z = B_1\mu_1 + B_2\mu_2, \;\; Z^\dagger = B_1^\dagger\mu_1 + B_2^\dagger\mu_2$$

where μ_k are the dipole moment vectors. As optical spectra can become rather congested,

we enhance the visibility of vibronic coupling effects by assuming that only monomer 1 is optically bright ($\mu_1 = 1$), while monomer 2 is optically dark ($\mu_2 = 0$). Straightforward evaluation of $I(\omega)$ and $R(\omega)$ now requires propagation of the dipole moment operator with the Hamiltonian H comprising three excitonic states and four vibrational modes. This can be done by standard basis-set or grid methods, but the actual computations are rather time consuming. Instead of employing more advanced computational techniques [18, 22, 45–48], here we partition the vibrations into the so-called "plus" and "minus" coordinates and momenta [14, 20, 21, 28, 39, 49]. As detailed in Appendix B, this procedure drastically simplifies calculations and reduces computational cost.

We show simulated absorption spectra $I(\omega)$ at a range of parameters in Fig. 1. Note that, while the spectra are plotted in arbitrary units, the total oscillator strength is conserved, since (Eq. (B6)) $\int_{-\infty}^{\infty} d\omega I(\omega) = 2\pi\mathcal{C}(0)$ [50]. The monomer spectrum (equivalent to the spectrum of a homo-dimer with the dipole coupling $\Delta = 0$) shown in panel (a) is simple, with an intense 0-0 transition and weak vibrational features at 195 cm^{-1} and 724 cm^{-1} corresponding to the fundamentals of the modes Ω_1 and Ω_2. Turning on the coupling in this completely degenerate dimer results in dramatic changes to the absorption spectrum, as seen in panel (a) of Fig. 1. While excitonic splitting and redistribution of oscillator strength is a consequence in any coupled dimer, it is clear that the inclusion of weakly coupled vibrations at each site has a substantial effect on the spectral shape. In particular, while a transition appears as expected at $E_1 = -\frac{1}{2}\delta_\epsilon$, the absorption peak expected at $E_2 = \frac{1}{2}\delta_\epsilon$ in a purely excitonic dimer instead appears as two equal intensity bands split almost symmetrically around the pure excitonic energy (indicated by vertical dashed lines). As illustrated in panel (b) of Fig. 1, this qualitative picture of a single low-frequency absorption feature in combination with split higher-frequency transitions prevails as the site energy ϵ_2 increases. It is clear, however, that as ϵ_2 increases the redistribution of oscillator strength is strongly suppressed. Concomitant with this suppression, the peak splitting increases, and the spectral lineshape tends towards that of a purely excitonic dimer with decoupled vibrations. Comparing the observed transition frequencies with those of the excitonic dimer is revealing. According to Eq. (12), we should expect strong transition frequency deviations only when vibronic coupling is strong – *i.e.* when conditions #1 and #2 are fulfilled. Plotting the frequency of the three lowest frequency transitions (hereafter, to states 1, 2, and 3) as a function of ϵ_2 in panels (c) and (d) corroborates this. The lowest

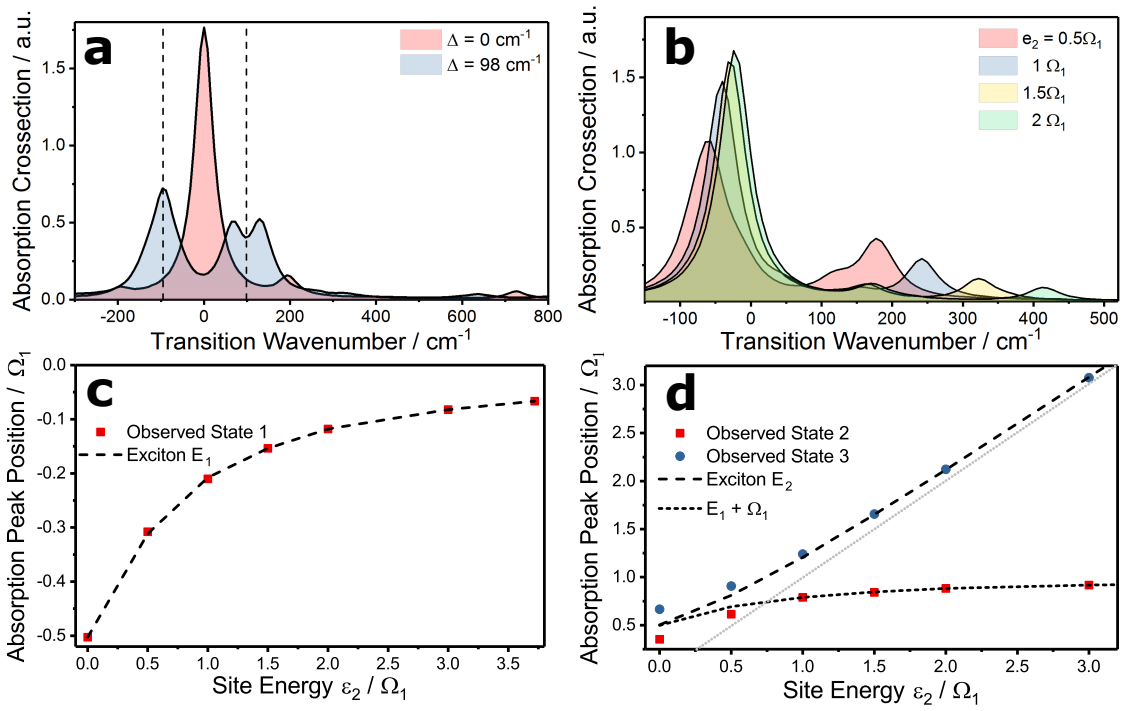

FIG. 1. **a)** Linear absorption spectra for homodimer with (blue) and without (red) dipole couplings Δ. **b)** Heterodimer absorption spectra as a function of the splitting ϵ_2 of monomer energies. Splitting energies given in units of the vibrational frequencies. **c)** The calculated position (in units of vibrational frequency Ω_1) of the lowest energy transition as a function of ϵ_2, compared with the expected position of the lowest energy exciton in a pure excitonic dimer (dashed line). **d)** The calculated position of the second (red) and third (blue) transition as a function of ϵ_2. For comparison we show the expected energy of the high-energy transition in an excitonic dimer (dashed line), the energy of the exciton in panel c plus a decoupled vibration Ω_1 (short dashed), and the peak-position = ϵ_2 diagonal line (gray line).

frequency transition – essentially to a zero-vibrational state – shows negligible deviations from the purely excitonic transition to E_1 (Fig. 1(c)). Similarly, at large ϵ_2 transitions to states 2 and 3 are virtually indistinguishable from transitions to a decoupled vibration and a pure excitonic state, respectively (Fig. 1(d)). At small ϵ_2, on the other hand, the situation is completely different: here, both transitions are strongly modulated by the interaction between electronic and vibrational degrees of freedom. This results in substantial shifts of the system eigenenergies, as predicted by Eq. (12). We note that vibronic interactions are also observable in the spectral region around Ω_2, but as the coupling strength is rather small

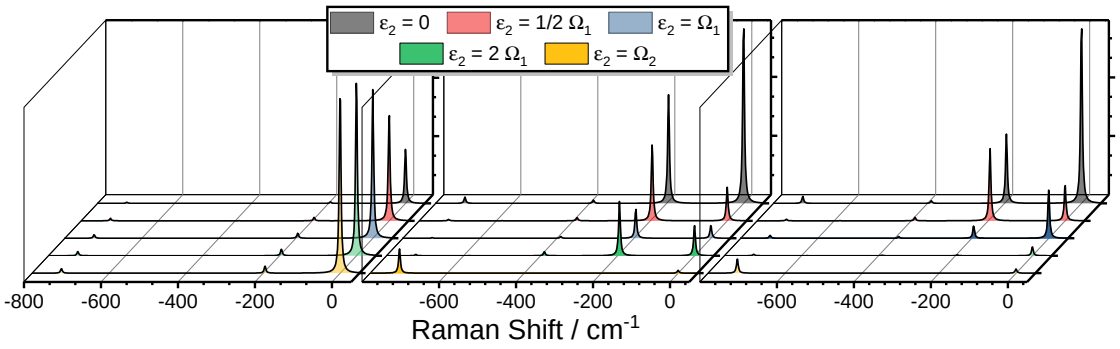

FIG. 2. Resonance Raman spectra as a function of site energies ϵ_2. Excitation resonant with the lowest energy state 1 (left panel), state 2 (middle panel), and state 3 (right panel).

relative to the energy gap, the resulting redistribution of oscillator strength is small, and the spectral evolution is much more subtle.

Due to the resonant interactions, one might expect that also the resonance Raman spectra show a substantial dependence on vibronic coupling. This is demonstrated in Fig. 2, where it is clear that the qualitative shapes also of vibrational spectra are strongly dependent on both the electronic structure and excitation frequency. We note that the observed vibrations are associated with the electronic ground-state [40, 51, 52], and are thus themselves not vibronic in character. As such, we do not observe *e.g.* frequency shifts upon excited-state electronic structure changes. Instead, the peak intensities – and their ratios – become reporters on vibronically coupled excited states through their dependence on the transition dipole moments.

The spectra acquired by excitation resonant with the lowest energy – and essentially purely excitonic – State 1 (Fig. 2, left panel) are simple. These are dominated by the Rayleigh line, as expected given the small Huang-Rhys factors of the chromophores, and the overall shape of the spectrum is virtually unaffected by the excited state structure. The observed change in signal intensity at increasing ϵ_2 simply reflects the redistribution of oscillator strength towards the lowest energy exciton as the effect of coupling decreases, as one would expect given the absorption spectra in Fig. 1(b). The character of states 2 and 3 is strongly dependent on vibronic coupling, as evident from the linear absorption spectra and Eq. (12). The vibronic coupling manifests itself as a strong dependence of the resonance Raman spectra – both in overall signal strength and in spectral shape – on ϵ_2 (see Fig. 2(b) and (c)).

The non-trivial changes in spectral shape can be illustrated by comparison of the homodimer with and without coupling (Fig. 3(a)). In the $\Delta = 0$ case, excitation resonant at Ω_1 results in a Raman spectrum dominated by this 195 cm^{-1} feature due to favorable Franck-Condon integrals. As we allow coupling between the sites, the states 2 and 3 take on partially electronic character due to the vibronic coupling, resulting in a less favorable Franck-Condon integral and decrease of Raman-to-Rayleigh scatter. The consequences of these mixing processes are, as illustrated by plotting the Ω_1 to Rayleigh line ratios in Fig. 3(b), highly non-trivial functions of the excited-state electronic structure with a maximum around $\epsilon_2/\Omega_1 \approx 0.5$. It is clear, however, that as ϵ_2 increases, the overall behavior tends towards that of the uncoupled dimer, with states 2 and 3 approaching a pure vibrational state and a pure excitonic state, respectively.

While a larger degree of vibrational character of a state thus seems to increase the relative intensity of particular lines in the resonance Raman experiment, estimation of the absolute magnitude of the signal is less simple. As is clearly demonstrated in Fig. 3(c), strong vibrational mixing (*i.e.* small ϵ_2) tend to increase the overall signal intensity in this model due to the redistribution of oscillator strength into the vibronically mixed higher-energy states. Finding the optimal parameters for enhancement of a particular mode thus becomes a non-trivial optimization problem, where the favorable Franck-Condon factors of a purely vibrational system must be weighed against the potentially significantly enhanced oscillator strength in the vibronically mixed situation.

VI. CONCLUSION

In the present work we have established, in the perturbative limit, the rigorous rules which govern coupling of excitonic and vibrational degrees of freedom in chromophore aggregates, and highlighted the consequences of such coupling for optical spectra. We have validated our analysis by the numerical simulations of optical spectra of a model dimer consisting of chromophores with two (low-frequency and high-frequency) vibrational modes. The compact analytical formula for the eigenvalues of the general exciton-vibrational Hamiltonian (in the leading second order) allowed us to define a generalized Huang-Rhys factor for molecular aggregates. Further, we could establish the required conditions for strong coupling of excitonic and vibrational degrees of freedom - conditions #1 and #2. The simultaneous fulfillment of

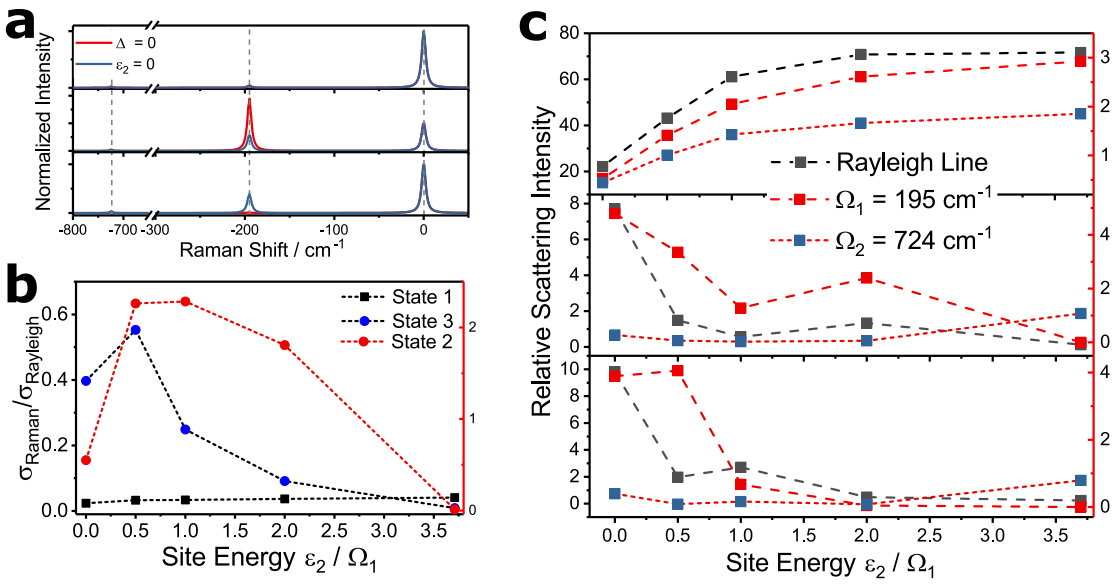

FIG. 3. **a)** The effect of electronic coupling on the Resonance Raman spectra a homodimer. Excitation into state 1 (top), state 2 (middle), and state 3 (bottom). **b)** The intensity ratio between Rayleigh scatter and the Ω_1 Raman line as a function of ϵ_2. Excitation frequencies resonant with the states noted in the panel. **c)** The intensity of the Rayleigh and Raman features as a function of ϵ_2. Excitation resonant with state 1 (top), state 2 (middle), and state 3 (bottom).

both of these ensures that excitonic and vibrational degrees of freedom are strongly coupled despite weak coupling in the individual constituent chromophores. Considering typical magnitudes of excitonic energies and dipole couplings in biological pigment-protein complexes, we predict that these conditions are only reasonably well fulfilled for relatively low-frequency (say $\lesssim 500$ cm^{-1}) vibrational modes. For higher-frequency modes the conditions are generally not fulfilled in natural systems, as the coupling becomes small relative to the energy-level splitting. These results qualitatively explain why only relatively low-frequency vibrational modes have been detected in time-domain experiments on aggregates such as the photosystem II reaction center [44], chlorosomes [53], the Fenna-Matthews-Olson complex [55, 56], as well as artificial light-harvesting J-aggregates [54].

ACKNOWLEDGMENTS

L. C. acknowledges support from a postdoctoral fellowship of the Alexander von Humboldt-Foundation. M. F. G. and W. D. acknowledge support from the Deutsche Forschungsgemein-

schaft through a research grant and through the DFG Cluster of Excellence Munich-Centre for Advanced Photonics (http://www.munich-photonics.de)

Appendix A: Evaluation of eigenenergies of the excitonic Hamiltonian

1. Second order perturbation theory

Consider a Hamiltonian

$$H = H_0 + V,$$

where H_0 is a certain zero-order Hamiltonian and V is a perturbation,

$$\| H_0 \| \gg \| V \| .$$

Let us introduce the eigenfunction representation for H_0,

$$H_0 |a\rangle = E_a^{(0)} |a\rangle .$$

Then the eigenenergies E_a of the total Hamiltonian H, up to the second order in V, are written as (see, e.g., Ref. [57])

$$E_a = E_a^{(0)} + V_{aa} + \sum_{b \neq a} \frac{|V_{ab}|^2}{E_a^{(0)} - E_b^{(0)}} \tag{A1}$$

where

$$V_{ab} = \langle a|V|b\rangle.$$

For the problem we are interested here V is real and

$$\langle a|V|a\rangle = 0. \tag{A2}$$

Hence

$$E_a = E_a^{(0)} + \sum_{b \neq a} \frac{V_{ab}^2}{E_a^{(0)} - E_b^{(0)}}. \tag{A3}$$

To evaluate Eq. (A3), it is convenient to rewrite it in the equivalent operator form:

$$E_a = E_a^{(0)} - i \lim_{\nu \to 0} \int_0^\infty e^{-\nu t} \langle a|e^{iH_0 t} V e^{-iH_0 t} V|a\rangle. \tag{A4}$$

2. Application to the Hamiltonian of Eq. (5)

Let us now set

$$H_0 = \mathcal{H}_e + \mathcal{H}_v, \;\; V = \mathcal{H}_{ev}.$$

Adopting the notation (9)-(11), we see that Eq. (A2) is fulfilled since $\langle\lambda| X_{k\alpha} |\lambda\rangle = 0$. It is further convenient to define the vibrational creation and annihilation operators $a_{k\alpha}$ and $a^\dagger_{k\alpha}$,

$$[a_{k\alpha}, a^\dagger_{k'\beta}] = \delta_{kk'}\delta_{\alpha\beta}, \tag{A5}$$

in terms of which

$$X_{k\alpha} = \frac{1}{\sqrt{2}}(a^\dagger_{k\alpha} + a_{k\alpha}), \;\; P_{k\alpha} = \frac{1}{\sqrt{2}}(a^\dagger_{k\alpha} - a_{k\alpha}). \tag{A6}$$

Hence Eq. (A4) assumes the form:

$$\mathcal{E}_{r\lambda} = \varepsilon_r + \omega_\lambda - \frac{i}{2}\sum_{k,n,n',k',m,m'=1}^{N_e}\sum_{\alpha,\beta=1}^{N_v} A^{nn'}_{k\alpha} A^{mm'}_{k'\beta} G \tag{A7}$$

where

$$G = \lim_{\nu\to 0}\int_0^\infty e^{-\nu t}\langle\lambda|\langle r| e^{iH_0 t} C^\dagger_n C_{n'} (a_{k\alpha} + a^\dagger_{k\alpha}) e^{-iH_0 t} C^\dagger_m C_{m'} (a_{k'\beta} + a^\dagger_{k'\beta}) |r\rangle |\lambda\rangle \, .$$

Since

$$[H_e, H_v] = 0 \tag{A8}$$

we can use the identities

$$e^{iH_0 t} C^\dagger_n = e^{i\varepsilon_n t} C^\dagger_n e^{iH_0 t}, \;\; e^{iH_0 t} C_n = e^{-i\varepsilon_n t} C_n e^{iH_0 t},$$

$$e^{iH_0 t} a^\dagger_{k\alpha} = e^{i\Omega_{k\alpha} t} a^\dagger_{k\alpha} e^{iH_0 t}, \;\; e^{iH_0 t} a_{k\alpha} = e^{-i\Omega_{k\alpha} t} a_{k\alpha} e^{iH_0 t},$$

which are the consequence of the Heisenberg equations of motion for excitonic and vibrational operators. Therefore,

$$G = \lim_{\nu\to 0}\int_0^\infty e^{-\nu t} e^{i(\varepsilon_n - \varepsilon_{n'})t} \langle\lambda|\langle r| C^\dagger_n C_{n'} (a_{k\alpha} e^{-i\Omega_{k\alpha} t} + a^\dagger_{k\alpha} e^{i\Omega_{k\alpha} t}) C^\dagger_m C_{m'} (a_{k'\beta} + a^\dagger_{k'\beta}) |r\rangle |\lambda\rangle \, .$$

Performing the time integral and employing Eq. (A5), we obtain

$$G = -\frac{1}{i}\langle r| C^\dagger_n C_{n'} C^\dagger_m C_{m'} |r\rangle \, \delta_{kk'}\delta_{\alpha\beta}\left[\frac{1 + n^\lambda_{k\alpha}}{\omega_{nn'} - \Omega_{k\alpha}} + \frac{n^\lambda_{k\alpha}}{\omega_{nn'} + \Omega_{k\alpha}}\right] \tag{A9}$$

where $\omega_{nn'}$ and $n^\lambda_{k\alpha}$ are given by Eqs. (13) and (14), respectively.

If we consider only singly excited excitonic states, then

$$|r\rangle = C_r^\dagger |0\rangle$$

($|0\rangle$ being the excitonic vacuum) and

$$\langle r|C_n^\dagger C_{n'} C_m^\dagger C_{m'} |r\rangle = \delta_{m'r}\delta_{nr}\delta_{n'm}. \tag{A10}$$

Then, combining Eqs. (A7), (A9) and (A10) we obtain Eq. (12).

Appendix B: Useful tricks with the dimer Hamiltonian

To simplify the calculations, we introduce the symmetrized (the superscript s) and anti-symmetrized (the superscript a) coordinates and momenta (cf. Refs. [14, 20, 21, 28, 39, 49]):

$$\begin{aligned} x_\alpha^s &= (X_{1\alpha} + X_{2\alpha})/\sqrt{2}, \;\; x_\alpha^a = (X_{1\alpha} + X_{2\alpha})/\sqrt{2}, \\ p_\alpha^s &= (P_{1\alpha} + P_{2\alpha})/\sqrt{2}, \;\; p_\alpha^a = (P_{1\alpha} + P_{2\alpha})/\sqrt{2}. \end{aligned} \tag{B1}$$

The inverse transformation reads:

$$\begin{aligned} X_{1\alpha} &= (x_\alpha^s + x_\alpha^a)/\sqrt{2}, \;\; X_{2\alpha} = (x_\alpha^s - x_\alpha^a)/\sqrt{2}, \\ P_{1\alpha} &= (p_\alpha^s + p_\alpha^a)/\sqrt{2}, \;\; P_{2\alpha} = (p_\alpha^s - p_\alpha^a)/\sqrt{2}. \end{aligned} \tag{B2}$$

After the insertion of Eqs. (B2) into Eq. (1) with $N_e = 2$, one obtains

$$H_v = H_v^s + H_v^a, \;\; H_{ev} = H_{ev}^s + H_{ev}^a.$$

Explicitly,

$$\begin{aligned} H_v^s &= \sum_{\alpha=1}^{N_v} \frac{\Omega_\alpha}{2} \left([p_\alpha^s]^2 + [x_\alpha^s]^2 \right), \\ H_v^a &= \sum_{\alpha=1}^{N_v} \frac{\Omega_\alpha}{2} \left([p_\alpha^a]^2 + [x_\alpha^a]^2 \right); \\ H_{ev}^s &= \left(B_1^\dagger B_1 + B_2^\dagger B_2 \right) h_{ev}^s, \\ H_{ev}^a &= \left(B_1^\dagger B_1 - B_2^\dagger B_2 \right) h_{ev}^a, \\ h_{ev}^s &= \sum_{\alpha=1}^{N_v} \Omega_\alpha \bar{\kappa}_\alpha x_\alpha^s, \;\; h_{ev}^a = \sum_{\alpha=1}^{N_v} \Omega_\alpha \bar{\kappa}_\alpha x_\alpha^a. \end{aligned}$$

In the above formulas,

$$\bar{\kappa}_\alpha = \kappa_\alpha/\sqrt{2}.$$

With these definitions, the Hamiltonian H decomposes into the sum of two commuting Hamiltonians,

$$H = H^s + H^a, \;\; [H^s, H^a] = 0. \tag{B3}$$

Explicitly,

$$H^s = H^s_{ev} + H^s_v, \tag{B4}$$

$$H^a = H_e + H^a_{ev} + H^a_v. \tag{B5}$$

The linear absorption spectrum is determined by the Fourier transform of the correlation function $\mathcal{C}(t)$ of the transition dipole moment operators [40],

$$I(\omega) = \mathrm{Re} \int_0^\infty dt e^{-t/\tau} e^{-i\omega t} \mathcal{C}(t), \tag{B6}$$

$$\mathcal{C}(t) = \mathrm{Tr}\left\{\rho_{eq} e^{iHt} Z e^{-iHt} Z^\dagger\right\}. \tag{B7}$$

Here $\mathrm{Tr}\{...\}$ is the trace over the excitonic and vibrational degrees of freedom and

$$\rho_{eq} = Z_{eq}^{-1} e^{-H_v/(k_B T)}$$

is the equilibrium vibrational distribution (k_B is the Boltzmann constant and T is temperature) and τ is the optical dephasing time. Making use of the fact that

$$e^{iH^s t} Z e^{-iH^s t} = e^{iH^s_v t} e^{-i(H^s_v + h^s_{ev})t} Z,$$

we obtain

$$\mathcal{C}(t) = \mathcal{C}^s(t)\mathcal{C}^a(t)$$

where

$$\mathcal{C}^s(t) = \mathrm{Tr}_s\left\{\rho^s_{eq} e^{iH^s_v t} e^{-i(H^s_v + h^s_{ev})t}\right\},$$

$$\mathcal{C}^a(t) = \mathrm{Tr}_a\left\{\rho^a_{eq} e^{iH^a t} Z e^{-iH^a t} Z^\dagger\right\}$$

Here $\mathrm{Tr}_s\{...\}$ is a trace over symmetric vibrational modes, $\mathrm{Tr}_a\{...\}$ is a trace over excitonic degrees of freedom and asymmetric vibrational modes and

$$\rho^s_{eq} = Z_s^{-1} e^{-H^s_v/(k_B T)}, \;\; \rho^a_{eq} = Z_a^{-1} e^{-H^a_v/(k_B T)}, \;\; \rho_{eq} = \rho^s_{eq}\rho^a_{eq}.$$

$\mathcal{C}^s(t)$ can be evaluated analytically as described e.g. in Ref. [40]:

$$\mathcal{C}^s(t) = e^{-g(t)}$$

where

$$g(t) = \sum_{\alpha=1}^{N_v} g_\alpha(t),$$

$$g_\alpha(t) = \frac{\bar{\kappa}_\alpha^2}{2}\left\{\coth\left(\frac{\Omega_\alpha}{2k_BT}\right)(1-\cos(\Omega_\alpha t)) + i\,(\sin(\Omega_\alpha t) - (\Omega_\alpha t))\right\}.$$

Hence only the antisymmetrized correlation function $\mathcal{C}^a(t)$ has to be computed numerically. It is governed by the Hamiltonian H^a which contains just a half of the original number of vibrational degrees of freedom. In the present case of $N_e = N_v = 2$, H^a has two vibrational modes.

Raman signals were computed by employing the partitioning (B3)-(B5) of the total Hamiltonian and using the Kramers-Heisenberg expression for Raman scattering [40].

---

[1] T. Renger, V. May, and O. Kühn, Phys. Rep. 343 (2001) 137.

[2] D. Abramavicius, B. Palmieri, D. V. Voronine, F. Šanda, and S. Mukamel, Chem. Rev. 109 (2009) 2350.

[3] T. Mirkovic, E. E. Ostroumov, J. M. Anna, R. van Grondelle, Govindjee, and G. D. Scholes, Chem. Rev. 117 (2017) 249.

[4] N. J. Cherepy, A. P. Shreve, L. J. Moore, S. G. Boxer, and R. A. Mathies, J. Phys. Chem. B 101 (1997) 3250.

[5] M. Wendling, T. Pullerits, M. A. Przyjalgowski, S. I. E. Vulto, T. J. Aartsma, R. van Grondelle, and H. van Amerongen, J. Phys. Chem. B 104 (2000) 5825.

[6] M. Rätsep and A. Freiberg, J. of Luminesc. 127 (2007) 251.

[7] D. Egorova, Chem. Phys. 347 (2008) 166.

[8] N. Christensson, H. F. Kauffmann, T. Pullerits, and T. Mančal, J. Phys. Chem. B 116 (2012) 7449.

[9] A. Chenu, N. Christensson, H. F. Kauffmann, and T. Mančal, Sci. Rep. 3 (2013) 2029.

[10] V. Butkus, D. Zigmantas, L. Valkunas, and D. Abramavicius, Chem. Phys. Lett. 545 (2012) 40.

[11] V. Butkus, L. Valkunas, and D. Abramavicius, J. Chem. Phys. 137 (2012) 044513.

[12] V. Butkus, L. Valkunas, and D. Abramavicius, J. Chem. Phys. 140 (2014) 034306.

[13] A. W. Chin, J. Prior, R. Rosenbach, F. Caycedo-Soler, S. F. Huelga, and M. B. Plenio, Nat. Phys. 9 (2013) 113.

[14] V. Tiwari, W. K. Peters, D. M. Jonas, Proc. Natl. Acad. Sci. USA 110 (2013) 1203.

[15] R. Tempelaar, T. L. C. Jansen, and J. Knoester, J. Phys. Chem. B 118 (2014) 12865.

[16] Y. Fujihashi, G. R. Fleming, and A. Ishizaki, J. Chem. Phys. 142 (2015) 212403.

[17] L. Valkunas, and D. Abramavicius, Photosynth. Res. 127 (2016) 33.

[18] M. Kess, G. Worth, and V. Engel, J. Chem. Phys. 145 (2016) 084305.

[19] J. D. Gaynor and M. Khalil, J. Chem. Phys. 147 (2017) 094202.

[20] V. Tiwari, W. K. Peters, and D. M. Jonas, J. Chem. Phys. 147 (2017) 154308.

[21] V. Tiwari and D. M. Jonas, J. Chem. Phys. 148 (2018) 084308.

[22] N. J. Hestand and F. C. Spano, Chem. Rev. 118 (2018) 7069.

[23] D. Egorova, M. Thoss, W. Domcke, and H. Wang, J. Chem. Phys. 119 (2003) 2761.

[24] A. V. Pisliakov, M. F. Gelin, and W. Domcke, J. Phys. Chem. A 107 (2003) 2657.

[25] J. A. Cina and G. R. Fleming, J. Phys. Chem. A 108 (2004) 11196.

[26] H. Hossein-Nejad and G. D. Scholes, New J. Phys. 12 (2010) 065045.

[27] F. C. Spano, Acc. Chem. Res. 43 (2010) 429.

[28] M. F. Gelin, L. Z. Sharp, D. Egorova and W. Domcke, J. Chem. Phys. 136 (2012) 034507.

[29] R. Borrelli and A. Peluso, Comput. Mol. Sci. 3 (2013) 542.

[30] C. Bruening, J. Wehner, J. Hausner, M. Wenzel, and V. Engel, Struct. Dyn. 3 (2016) 043201.

[31] P. Malý, O. J. G. Somsen, V. I. Novoderezhkin, T. Mančal, and R. van Grondelle, ChemPhysChem 17 (2016) 1356.

[32] X. Li, G. G. Gurzadyan, M. F. Gelin, W. Domcke, C. Gong, J. Liu and L. Sun, J. Phys. Chem. C 122 (2018) 23321.

[33] M. Schröter, S. D. Ivanov, J. Schulze, S. P. Polyutov, Y. Yan, T. Pullerits, and O. Kühn, Phys. Rep. 567 (2015) 1.

[34] C. Curutchet and B. Mennucci, Chem. Rev. 117 (2017) 294.

[35] S. J. Jang and B. Mennucci, Rev. Mod. Phys. 90 (2018) 035003.

[36] V. Chernyak and S. Mukamel, J. Chem. Phys. 105 (1996) 4565.

[37] S. Mukamel and D. Abramavicius, Chem. Rev. 104 (2004) 2073.

[38] W. M. Zhang, T. Meier, V. Chernyak, and S. Mukamel, J. Chem. Phys. 108 (1998) 7763.

[39] R. L. Fulton and M. Gouterman, J. Chem. Phys. 41 (1964) 2280.

[40] S. Mukamel, *Principles of Nonlinear Optical Spectroscopy*. Oxford University Press, New York (1995).

[41] R. Borrelli, M. Di Donato, and A. Peluso, Comput. J. Chem. Theory Comput. 3 (2007) 673.

[42] J. Adolphs and T. Renger, Biophys. J. 91 (2006) 2778.

[43] J. Moix, J. Wu, P. Huo, D. Coker, and J. Cao, J. Phys.Chem. Lett. 2 (2011) 3045.

[44] F. D. Fuller, J. Pan, A. Gelzinis, V. Butkus, S. S. Senlik, D. E. Wilcox, C. F. Yocum, L. Valkunas, D. Abramavicius, and J. P. Ogilvie, Nat. Chem. 6 (2014) 706.

[45] R. Borrelli and M. F. Gelin, Sci. Rep. 7, 9127 (2016).

[46] L. Chen, M. F. Gelin, W. Domcke, and Y. Zhao, J. Phys. Chem. Lett. 9 (2018) 4488.

[47] L. Chen, R. Zheng, Q. Shi, and YiJing Yan, J. Chem. Phys. 132 (2010) 024505.

[48] D. M. Monahan, L. Whaley-Mayda, A. Ishizaki, and G. R. Fleming, J. Chem. Phys. 143 (2015) 065101.

[49] M. F. Gelin, D. Egorova, and W. Domcke, Phys. Rev. E 84 (2011) 041139.

[50] R. Gordon, Adv. Magn. Res. 3 (1968) 1.

[51] Note that femtosecond stimulated Raman spectroscopy reveals dephasing-free Raman-like vibrational peaks both in the ground and excited electronic states [52].

[52] M. F. Gelin, W. Domcke, and B. J. Rao, J. Chem. Phys. 144 (2016) 184307.

[53] J. Dostál, T. Mančal, F. Vácha, J. Pšenčík, and D. Zigmantas, J.Chem. Phys. 140 (2014) 115103.

[54] J. Lim, D. Paleček, F. Caycedo-Soler, C. N. Lincoln, J. Prior, H. von Berlepsch, S. F. Huelga, M. B. Plenio, D. Zigmantas and J. Hauer, Nature Comm. 6 (2015) 7755.

[55] M. Maiuri, E. E. Ostroumov, R. G. Saer, R. E. Blankenship, and G. D. Scholes, Nat. Chem. 10 (2018) 177.

[56] E. Thyrhaug, R. Tempelaar, M. J. P. Alcocer, K. Zidek, D. Bina, J. Knoester, T. L. C. Jansen, and D. Zigmantas, Nat. Chem. 10 (2018) 780.

[57] L. D. Landau and L. M. Lifshitz, *Quantum Mechanics*. Pergamon Press, Oxford (1965).